UPGRADE OF A PROTON THERAPY EYE TREATMENT NOZZLE USING A CYLINDRICAL BEAM STOPPING DEVICE FOR ENHANCED DOSE RATE PERFORMANCES

E. Gnacadja*, C. Hernalsteens[1], N. Pauly, R. Tesse, E. Ramoisiaux, M. Vanwelde

Service de Métrologie Nucléaire, Université libre de Bruxelles, Brussels, Belgium

[1]also at CERN, Geneva, Switzerland

Abstract

Proton therapy is a well established treatment method for ocular cancerous diseases. General-purpose multi-room systems which comprise eye-treatment beamlines must be thoroughly optimized to achieve the performances of fully dedicated systems in terms of depth-dose distal fall-off, lateral penumbra, and dose rate. For eye-treatment beamlines, the dose rate is one of the most critical clinical performances, as it directly defines the delivery time of a given treatment session. This delivery time must be kept as low as possible to reduce uncertainties due to undesired patient movement. We propose an alternative design of the Ion Beam Applications (IBA) Proteus Plus (P+) eye treatment beamline, which combines a beam-stopping device with the already existing scattering features of the beamline. The design is modelled with Beam Delivery SIMulation (BDSIM), a Geant4-based particle tracking and beam-matter interactions Monte-Carlo code, to demonstrate that it increases the maximum achievable dose rate by up to a factor 3 compared to the baseline configuration. An in-depth study of the system is performed and the resulting dosimetric properties are discussed in detail.

INTRODUCTION

The use of proton beams to treat ocular tumors is well established [1–3]. The optimization of high energy multi-room proton therapy systems to allow ocular tumors treatment poses many challenges compared to dedicated low energy facilities. The key point of the design of such systems is the trade-off that must be found between a small depth-dose distal fall-off [1] (DFO, typically below 2 mm) and a high dose rate (often required to be at least equal to 15 Gy/min) in order to minimize treatment delivery time. Indeed, as eye tumors depths often vary from 5 to 35 mm, the beam nominal energy of high energy systems must be reduced from 250 MeV to 70 MeV or less prior to additional range shifting inside of a dedicated eye nozzle. As this energy degradation unevitably leads to a significant energy spread, momentum slits must be positioned at a location of high dispersion to intercept the more energetic particles and reduce the DFO of the dose deposition profiles. Such particles interception directly affects the transmission of the beamline, leading to a huge limitation on the dose rate performances of the system.

The Ion Beam Applications (IBA) eye treatment beamline, so-called "eyeline", is an example of such a high energy system, in which the beam is produced at a nominal energy of 230 MeV. The IBA eyeline has been previously designed [4]

* eustache.gnacadja@ulb.be
[1] The distal fall-off is defined as the difference between the 20 % and 80 % dose points on the distal side of the Bragg peak: DFO = $R_{80} - R_{20}$.

and experimentally optimized with an energy of 105 MeV at the nozzle entrance [5], leading to a maximum dose rate of 30 Gy/min, but with a DFO of only 3.2 mm. More recently, the different steps toward a numerical optimization for a smaller DFO (below 2 mm) has been presented in detail in [6], using Beam Delivery SIMulation (BDSIM) [7]. BDSIM is a geant4 based particle tracking and beam-matter interactions simulation code, that has already proven its ability to model low energy proton therapy systems [8]. This smaller DFO requirement forced the reduction of the nominal energy at the nozzle entrance from 105 to 80 MeV, leading to a smaller maximum achievable dose rate. Table 1 summarizes the clinical performances required during the optimization presented in [6].

Table 1: The clinical requirements (minimum range (R_{min}), maximum range (R_{max}), DFO, Flatness, Lateral Penumbra (LP) and Dose Rate (DR)) imposed on the dosimetric properties of the IBA passive scattering eyeline.

R_{min} (mm)	R_{max} (mm)	DFO (mm)	Flatness (%)	LP (mm)	DR (Gy/min)
5	35	< 2	< 2	< 1.5	> 15

As discussed in [6], two designs of the IBA eyeline were studied. The first design only uses the scattering and range shifting features of the system to optimize the nozzle, with at the end a maximum achievable dose rate of 17 Gy/min. The second, alternative design combines a cylindrical, lead material beam stopper, with the scattering features of the nozzle to achieve a transversally flat dose profile. Figure 1 illustrates the BDSIM model of the nozzle as designed with this cylindrical beam stopping device.
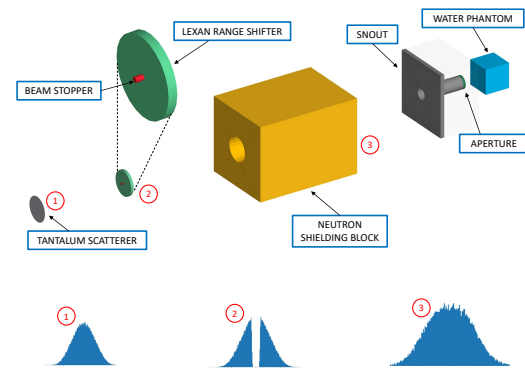

Figure 1: BDSIM model of the IBA eye treatment nozzle as designed with a cylindrical beam stopping device.

MC8: Applications of Accelerators, Technology Transfer and Industrial Relations
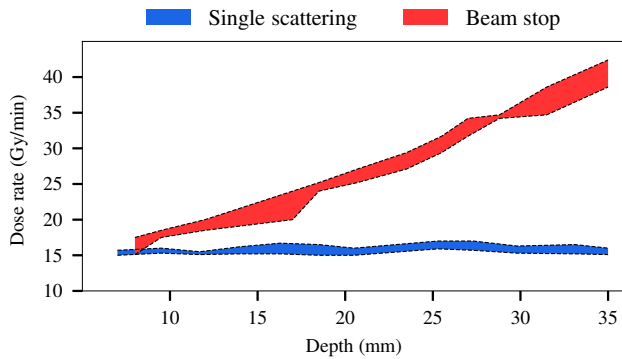
U01: Medical Applications

Figure 2: Evolution of the dose rate in function of clinical range, as calculated for the single scattering (green) and the beam stop (red) designs in [6]. The maximum achievable dose rate with the beam stopper design is 42.4 Gy/min, while the single scattering maximum value is around 17 Gy/min.

The beam first interacts with a thin 150 μm-thick Tantalum foil. Thanks to the high Z and high density of this Tantalum foil, a significant, randomly distributed transverse angle is given to the particles. As the beam propagates along the nozzle after this interaction, the transverse angles are converted into position and the beam size increases. After a distance of 35.5 cm, the beam crosses the lead beam stopper, which has a thickness of 10 mm. Such thickness is enough to stop all particles that cross the beam stopper, meaning that a hole is created in the middle of the beam distribution just after this interaction. Then the remaining particles continue to propagate on a distance of 165 cm up to isocenter. As the beam propagates, the hole is progressively filled by the particles due to their transverse angle, and a transversally flat profile is obtained at isocenter.

The design parameters obtained in [6] (scattering foil, beam stopper radius and position) when optimizing the nozzle with the beam stopper are summarized in Table 2.

Table 2: The design parameters of the nozzle when used with a beam stopping device. A 12 mm thick Lexan range shifter, placed just downstream of the beam stopper, is used to fix the maximum clinical range to 35 mm.

Ta thick. (mm)	Le thick. (mm)	Radius (mm)	Thick. (mm)	D_{FS-BS} (cm)
0.15	12	3.6	10	35.5

Figure 2 shows the results of the dose rate optimization using both designs, as obtained in [6]. We can observe that the beam stopper design allows achieving a maximum dose rate of 42.4 Gy/min, for the maximum clinical range of 35 mm. On the other hand, as the range decreases, the dose rate also decreases due to the fact that range shifting also induces scattering, leading to beam losses along the nozzle.

The aim of this paper is to investigate the possibility of further increasing the dose rate values at shallow depths (below 20mm) by changing the nominal energy at the nozzle entrance from 80 to 90 MeV in this interval. The goal is to benefit from the difference in beamline transmission between these two energies (1.15% at 80 MeV, 2.23% at

90 MeV) to restore dose rate values that are higher than 20 Gy/min across all the treatment range interval. After discussing the detailed numerical model of the nozzle, the design parameters that allow obtaining a transversally flat profile at isocenter are presented. Then the main simulation results (lateral and depth dose profiles, penumbra and dose rate in function of depth) are discussed in detail. Finally, the impact of the energy switching on the DFO is assessed for a full modulated Spread-Out Bragg Peak (SOBP) which has a maximum range of 20 mm.

SIMULATION RESULTS

Figure 3 shows a comparison between the single scattering and the beam stopper designs, for the same nominal energy of 80 MeV at the entrance of nozzle. As can be seen, the maximum dose is almost 3 times higher for the beam stopper design compared to the single scattering solution.
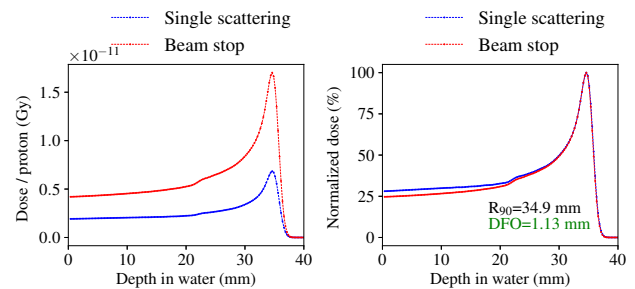

Figure 3: Bragg peaks simulated for a clinical range of 35 mm with the single scattering (blue) and the beam stopper (red) designs. The dose per primary proton (left) illustrates the dose rate improvement by a factor of 3 with the beam stopper design. After normalization (right), the beam stopper design exhibits a dose at skin which is almost 5% smaller than with the single scattering design.

Figure 4 shows a comparison of the lateral profiles obtained for the single scattering and the beam stopper design.

We observe that the clinical properties are the same for both designs in the irradiation field. At skin, the lateral dose tails (delivered outside of the irradiation field) are more significant for the single scattering design than with the beam stopper, meaning that the latter allows giving a smaller dose to shallow healthy tissues.

Figure 5 compares the evolution of the lateral penumbra with the clinical range for the two designs. Both exhibit similar behaviour, showing an increase of the penumbra with the range, as the protons are scattered in water.

In order to maintain the dose rate higher than 20 Gy/min over all the treatment range interval, a nominal energy of 90 MeV was selected for clinical ranges from 5 to 20 mm. Figure 6 shows a comparison between the estimated dose rate values with only 80 MeV and the results obtained when switching to 90 MeV for ranges smaller than 20 mm. We can clearly observe a significant jump in the dose rate curve at 20 mm for the solution that mixes 80 and 90 MeV. The jump is then followed by a decrease but the absolute minimum of the dose rate remains higher than 20 Gy/min.
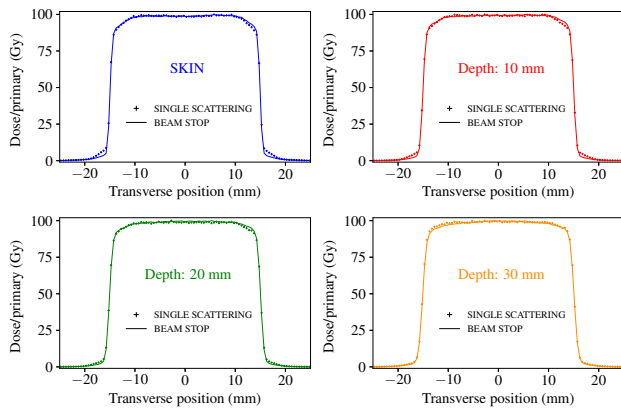
Figure 4: Lateral dose profiles at 4 different depths (skin, 10, 20 and 30 mm) in water. The single scattering and the beam stopper designs have similar clinical properties in the irradiation field. At skin we can observe slightly smaller lateral dose tails for the beam stopper design.

Figure 6: Dose rate values evaluated in function of the clinical range. The results when using a nominal energy of 80 MeV from 5 to 35 mm are shown in orange, while the green curve shows the results obtained when switching to 90 MeV for shallow depths (below 20 mm).
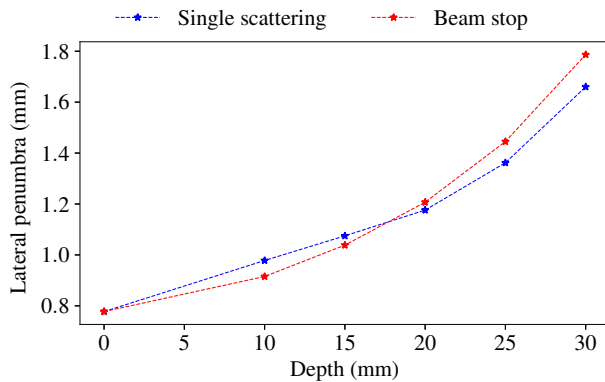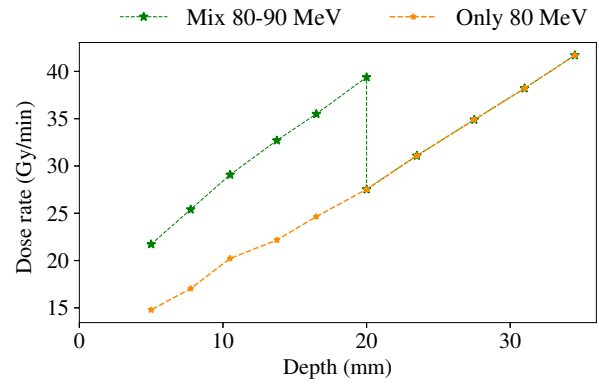

Figure 5: Lateral penumbra in function of the clinical range for the single scattering (blue) and the beam stopper (red) designs. An increase of the penumbra from 0.8 to around 1.8 mm is observed for both designs.
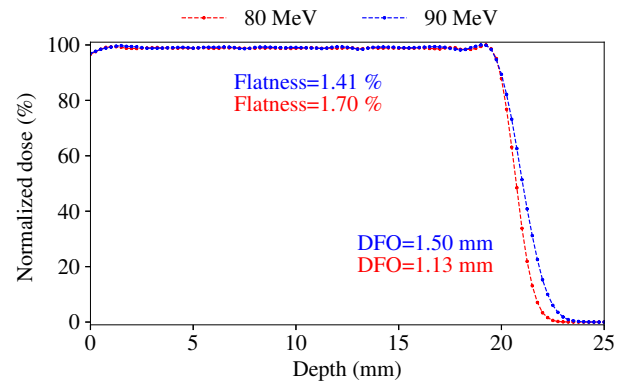

Figure 7: The full-modulation SOBPs for a clinical range of 20 mm, at 80 MeV (red) and at 90 MeV (blue). The flatness of both curves remains below the 2% limitation. At 90 MeV, a slightly higher DFO is observed due to the energy spread induced by the additional range shifting required inside of the nozzle.

On the other hand, the DFO is expected to inevitably increase as we need more range shifting inside of the nozzle to set the Bragg peaks at the same ranges as with a nominal energy of 80 MeV. Such DFO increase can be observed in Fig. 7, which compares the SOBPs obtained for the two different energies for a maximum clinical range of 20 mm. The DFO increases from 1.13 mm at 80 MeV to 1.5 mm at 90 MeV. However, it remains smaller than the limitation of 2 mm presented in Table 1, meaning that the proposed upgrade does not have a clinically significant impact on the DFO of the system.

deposition profile at isocenter. Starting from the previous results presented in [6] with a single nominal energy of 80 MeV at the entrance of the nozzle, we demonstrate that switching from 80 to 90 MeV for shallow depths (< 20 mm) allows to further optimize the dose rate and restore values obtained at larger depths (>20 mm). A minimum dose rate of 20 Gy/min is obtained across all the required treatment range interval (from 5 to 35 mm). Moreover, we show that the upgrade only induces an increase of 0.4 mm to the DFO, which reachs a maximum of 1.5 mm at a depth of 20 mm. As this value remains smaller than the limitation of 2 mm, the upgrade still fulfils all the targeted clinical requirements for the system.

CONCLUSION

We present in this paper an upgrade of the design of the IBA passive scattering ocular tumors treatment beamline using a beam stopping device. This design combines the existing scattering features of the beamline with a cylindrical, 10 mm thick beam stopper to provide a transversally flat dose

ACKNOWLEDGEMENTS

REFERENCES

[1] P. Jovanovic *et al.*, "Ocular melanoma: An overview of the current status," *Int. J. Clin. Exp. Pathol.*, vol. 6, no. 7, pp. 1230–1244, 2013, `pmid:23826405`.

[2] B. Damato *et al.*, "Proton beam radiotherapy of uveal melanoma," *Saudi J. Ophthalmol.*, vol. 27, no. 3, pp. 151–157, 2013, `doi:10.1016/j.ijrobp.2005.01.016`, `doi:10.1016/j.ijrobp.2005.01.016`

[3] E. S. Gragoudas *et al.*, "Proton irradiation of small choroidal malignant melanomas," *Am. J. Ophthalmol.*, vol. 83, no. 5, pp. 665–673, 1977, `doi:10.1016/0002-9394(77)90133-7`, `doi:10.1016/0002-9394(77)90133-7`

[4] D. Prieels, "Calculations and design considerations of the nozzle dedicated to eye irradiation," Ion Beam Applications, Tech. Rep., 2006.

[5] R. Slopsema *et al.*, "Dosimetric properties of a proton beamline dedicated to the treatment of ocular disease," *Med. Phys.*, vol. 41, no. 1, p. 011 707, 2014, `doi:10.1118/1.4842455`, `doi:10.1118/1.4842455`

[6] E. Gnacadja *et al.*, "Optimization of proton therapy eye-treatment systems toward improved clinical performances," *Phys. Rev. Research*, vol. 4, no. 1, p. 013 114, 2022, `doi:10.1103/PhysRevResearch.4.013114`, `doi: 10.1103/PhysRevResearch.4.013114`

[7] L. J. Nevay *et al.*, "BDSIM: An accelerator tracking code with particle–matter interactions," *Comput. Phys. Commun.*, vol. 252, p. 107 200, 2020, `doi:10.1016/j.cpc.2020.107200`, `doi:10.1016/j.cpc.2020.107200`

[8] C. Hernalsteens *et al.*, "A novel approach to seamless simulations of compact hadron therapy systems for self-consistent evaluation of dosimetric and radiation protection quantities," *EPL*, vol. 132, no. 5, p. 50 004, 2020, `doi:10.1209/0295-5075/132/50004`, `doi:10.1209/0295-5075/132/50004`